Astron. Astrophys. 251, 276–284 (1991)

ASTRONOMY AND ASTROPHYSICS

VLA observations of solar active regions at 6 and 20 cm

C. E. Alissandrakis[1], M. R. Kundu[2], and K. R. Shevgaonkar[3]

[1] Section of Astrophysics, Astronomy and Mechanics, Department of Physics, University of Athens, Greece
[2] Astronomy Program, University of Maryland, USA
[3] Indian Institute of Astrophysics, Bangalore, India

Received February 20, accepted May 13, 1991

Abstract. We present high resolution observations of two active regions at 6 and 20 cm over a period of 5 days, together with Hα and photospheric magnetic fields. The large scale emission at 20 cm is associated with the Hα plage. In one region the strongest source was over the neutral line, near the tip of an active region filament, which indicates that the emission probably originated in small scale coronal loops. In the second region the peak of the emission was near a well developed sunspot. Neither region showed evidence of large scale loops joining their preceding and following parts. Several other sources were observed at 20 cm; a source associated with an Hα plage region crossed by a filament and one associated with a small bipolar region are briefly discussed. The 6 cm emission from a well developed spot showed clearly the characteristics expected from gyroresonance model computations. The detailed shape of the source shows that the magnetic field of the spot was not potential. The sense of the required electric current is the same as that inferred from the analysis of chromospheric observations.

Key words: sun: radio radiation – sun: activity – sun: sunspots

1. Introduction

High resolution observations of solar active regions in the microwave domain have been made using large arrays such as the Westerbork Synthesis Radio Telescope (WSRT) and the Very Large Array (VLA) for more than a decade (e.g. Kundu et al. 1977; Kundu et al. 1981; Alissandrakis & Kundu 1984; Lang & Willson 1982; Chiuderi-Drago et al. 1977). These observations have shown that the slowly varying component of the sun's microwave emission is associated with sunspots, plages and regions of transverse magnetic fields or neutral lines. The strong sunspot-associated component which dominates the emission around 6 cm, with brightness temperatures of up to a few million degrees, has been generally interpreted as due to low harmonics of gyroresonance radiation. The weaker and diffuse low T_b ($\leq 10^5$ K) sources associated with chromospheric plages have usually been interpreted as due to thermal free-free emission from the transition region and the corona above active regions. The microwave sources with $T_b \geq 10^6$ K sometimes associated with regions of transverse magnetic fields are difficult to understand in terms of low harmonic gyroradiation (Kundu & Alissandrakis 1984). It is possible that such sources are due to a low level, quasi steady, non-thermal emission (Chiuderi-Drago & Melozzi 1984; Akhmedov et al. 1986). Non-thermal emission may also account for very bright sources associated with rapid changes in the magnetic field (Chiuderi-Drago et al. 1987).

Observations made with a few arc second resolution have shown that microwave sources associated with isolated sunspots can be fairly simple, with the total intensity structure agreeing approximately with the size of the penumbra. This structure can be understood in terms of thermal gyroresonance (g-r) emission in a plane-parallel, hydrostatic atmosphere. The circular polarization structure on the other hand is more complicated. For example, Alissandrakis & Kundu (1982) and Lang & Willson (1982) discovered that the circular polarization was higher at the edge of the total intensity source, forming a "ring" or "horseshoe" structure. This radio ring structure above a sunspot has been interpreted as due to a combination of g-r emission at the 2nd and 3rd harmonic. Occasionally the total intensity structure shows departures from the plane parallel assumption. The existence of cool material above the sunspot has been inferred from 6 cm observations (Alissandrakis & Kundu 1982) and simultaneous SMM soft X-ray observations (Strong et al. 1984; Siarkowski et al. 1989).

Of more practical importance have been the model computational studies of the slowly varying component as done over the past several years, for example by Gelfreikh & Lubyshev (1979), Alissandrakis (1980), Alissandrakis et al. (1980) & Krüger et al. (1985). Basically one compares the computed total intensity and polarization maps with the observed ones, and identifies which low order harmonic (2nd or 3rd) of the gyrofrequency is the dominant contributor to the radio emission. This in turn leads to a determination of magnetic field strength in the transition region and the corona. Alissandrakis & Kundu (1984) extended such model computations still further and obtained additional information about the coronal magnetic fields. Specifically, they compared the structure of one spot-associated source as well as its center-to-limb variation with model computations; they were able to identify features on the radio maps such as the region where the magnetic field is directed along the line of sight. Using a new method of analysis they mapped the vertical as well as the horizontal component of the sunspot magnetic field at specific locations in the low corona. This is clearly an improvement over the existing models of radio emission from active regions. Additional information about the scale height of the magnetic field

Send offprint requests to: C. E. Alissandrakis

Table 1. VLA observations

Date (1985)	Start (UT)	End (UT)	Duration	Frequency (MHz)	Pointing	Beam size (arc sec)
July 31	00:04	01:06	1:02	1446.15	N05 E13	30.2×15.0
	19:49	01:29	5:40	1446.15	N05 E07	17.6×14.2
	20:00	01:40	5:40	4866.35	S13 E43	5.3×4.4
August 1	13:40	16:52	3:12	1496.15	N05 E07	18.3×15.7
August 2	13:56	15:12	1:16	1446.15	N06 E05	23.8×16.8
	13:40	15:12	1:21	4866.35	N06 E05	8.0×4.9
	16:00	23:34	7:34	1446.15	N05 E06	17.4×16.8
	15:36	23:50	8:14	4866.35	S15 E16	4.3×3.9
August 3	14:00	23:35	9:35	1496.15	N05 E06	14.1×11.5
	13:37	00:10	10:55	4816.35	S14 E03	4.4×4.2

can be provided by spectral observations (Akhmedov et al. 1982; Krüger et al. 1986).

At 20 cm the emission comes from a more extended region, of about the same size as the plage (Chiuderi-Drago et al. 1977; Shevgaonkar & Kundu 1985). Sunspot-associated emission is not prominent, apparently because free-free emission from regions of moderate magnetic field strength becomes important as the wavelength increases. Several observers (Lang et al. 1982; McConnel & Kundu 1983) have reported the presence of large scale loops between the leading and the trailing parts of active regions. More recently, Gary & Hurford (1987) showed the transition from sunspot-associated emission at short centimeter wavelengths to loop associated emission around 20 cm. It should be noted however that, due to the relatively poor spatial resolution at 20 cm, plage and loop-associated emission cannot easily be distinguished in regions which are not close to the limb.

In order to make further advances in model computations of coronal magnetic fields and thereby in a detailed understanding of the generating mechanisms of active region emission, simultaneous high spatial resolution observations in various spectral domains (radio, X-ray, ultraviolet and optical) are needed. An excellent opportunity for such coordinated observations arose when the Spacelab 2 mission with several important experiments including the High Resolution Telescope and Spectrograph (HRTS) of NRL and the Solar Optical and Ultraviolet Polarimeter (SOUP) of Lockheed was flown in July-August of 1985. Simultaneous microwave (6 and 20 cm) observations were obtained with the VLA for several days during the Spacelab 2 mission during which HRTS was operating. However, the VLA observations ended (August 3) just before the SOUP started operating (August 4). In this paper, we present the VLA microwave observations obtained during the period July 30-August 3, 1985. In a subsequent paper, we shall use the radio data along with the HRTS data, in order to derive an empirical model of the active regions under study.

2. Observations

The observations were obtained daily from July 30 (actually ~0:30 UT of July 31) to August 3 (Table 1). In the L-band (20 cm) the field of view covers the entire sun and the instrument was pointed near the center of the disk. Thus two active regions, NOAA 4680 (northern hemisphere) and NOAA 4682 (southern hemisphere) were observed, as well as some other plage associated sources. In the C-band (6 cm) the field of view is limited to ~10′, thus it was not possible to observe both regions at the same time. Observations of the active region 4682 were obtained on July 31, August 2 and August 3 and of the region 4680 on August 2. During these periods the VLA was in the C configuration; it operated in a basic cycle of 30 min, with 10 min of L-band solar observations, 10 min of C-band solar observations, 5 min of C-band calibrator observations and 5 min of L-band calibrator observations. In general, the resolution was ~17″ in the L-band and ~4″ in the C-band, except on July 30 when the observing period was much shorter (~1 hour) and the resolution was only 30″ by 15″ in the L-band.

A problem in the VLA solar pointing was found after these observations were obtained: the parallax correction had the wrong sign. This translates to a shift of the source with respect to the VLA phase center at a rate of about 4″/hour near central meridian transit and a total shift of ~14″ for a source observed from −6 hours to 6 hours. The shift is much larger than the size of the beam at 6 cm, therefore we computed several short maps during the day which were subsequently shifted and averaged to give the full day maps; ten short maps were used to produce the July 31 C-band map and three for the August 2 and 3 maps.

When comparing the 6 and 20 cm maps, one must keep in mind that they show different spatial scales. In addition to the obvious difference of resolution, the L-band maps are more sensitive to large scale structures than the C-band maps, with consequences on the detection of the plage-associated emission. The quiet sun does not show up even in the L-band maps (Fig. 1), but here we have the additional effect of the limited dynamic range, combined with the intense active region emission.

For a better understanding of the cm-λ emission it is important to have additional information about the photospheric magnetic field and the chromospheric structure. Hα photographs were provided by the Sacramento Peak Observatory (SPO) and magnetograms by the Marshall Space Flight Center (MSFC, both longitudinal and transverse), the Kitt Peak National Obser-

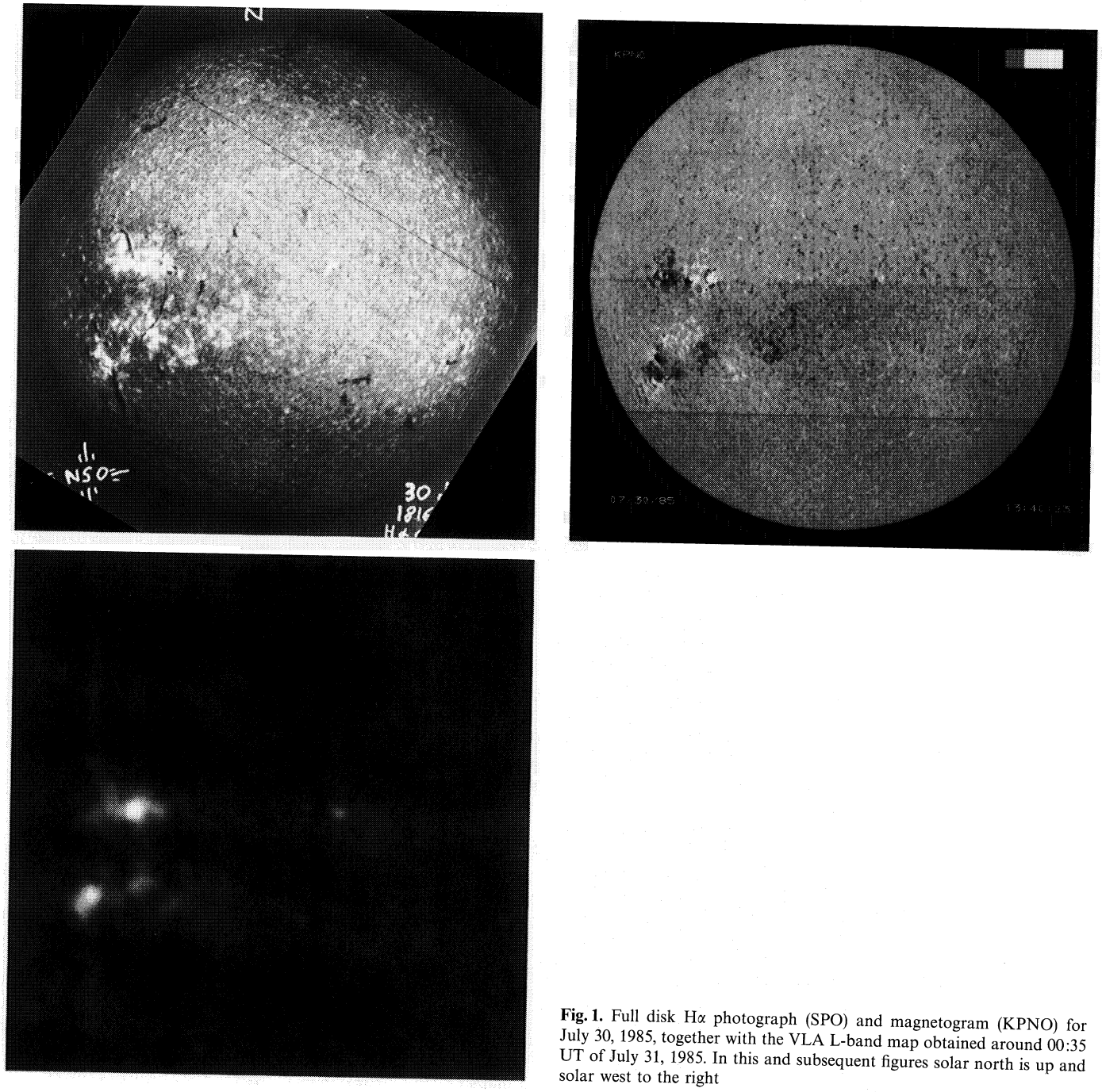

Fig. 1. Full disk Hα photograph (SPO) and magnetogram (KPNO) for July 30, 1985, together with the VLA L-band map obtained around 00:35 UT of July 31, 1985. In this and subsequent figures solar north is up and solar west to the right

vatory (KPNO) and the Observatoire de Paris, Meudon. Sunspot information was obtained from Solar Geophysical Data (SGD).

3. Overall view of the sun

Figure 1 shows for July 30, 1985 the full-disk images in Hα (SPO), the L-band (VLA) and the KPNO magnetogram. The most prominent features of the radio emission are the two main active regions, NOAA 4680 in the northern hemisphere and NOAA 4682 in the southern hemisphere. These active regions and their evolution will be described in detail in the rest of this paper. Here we shall briefly discuss the various features of the solar disk during our observing period.

The L-band radio emission associated with the region 4680 consists of an intense compact component surrounded by some diffuse emission. The compact component lies to the south of the prominent active region filament and close to a bright plage. The southern radio source (L-band) also consists of an intense compact component associated with the north part of the active region where a well developed spot is located; it also has an extensive diffuse low-level component which appears to be primarily plage-associated emission.

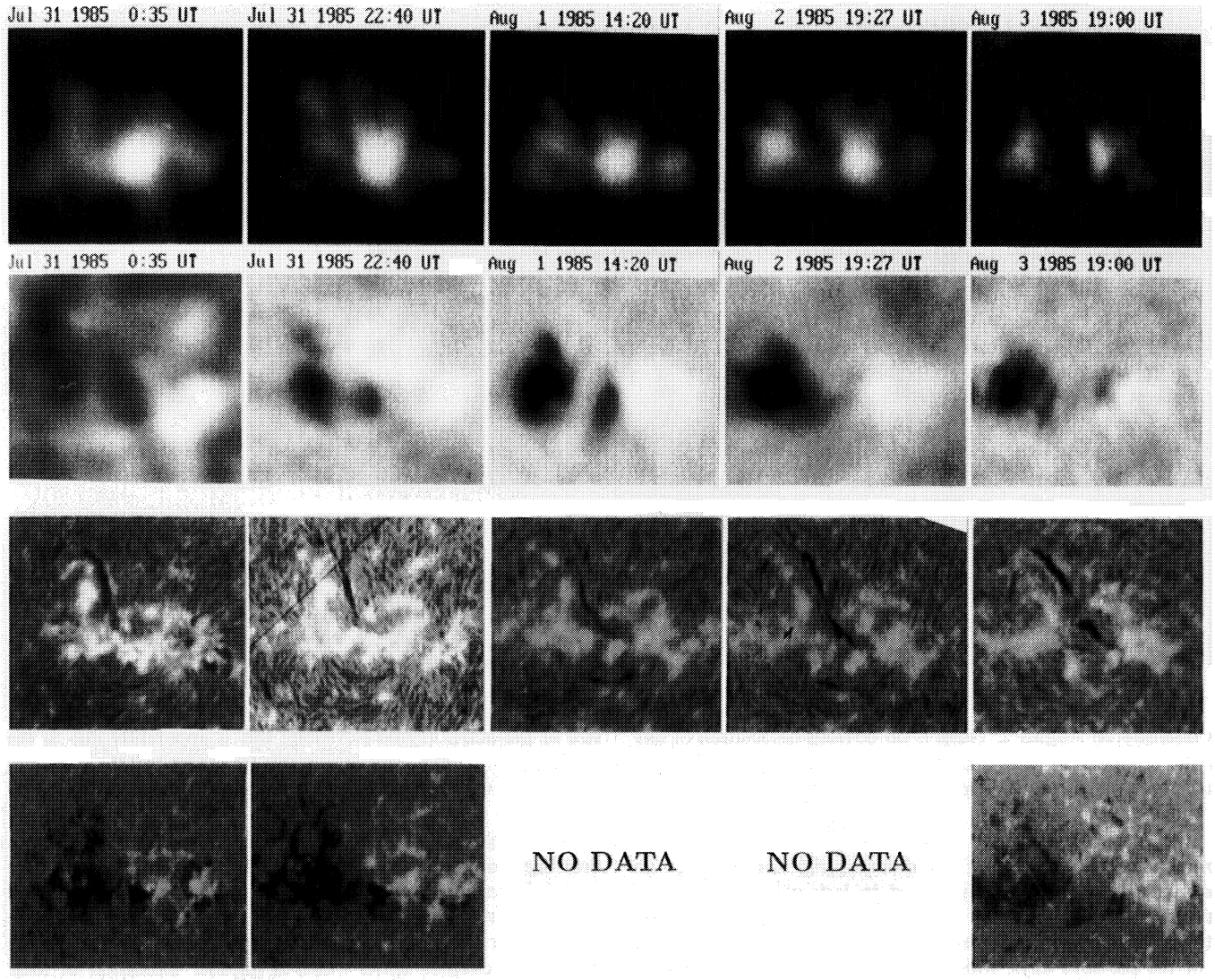

Fig. 2. Daily VLA maps of the Northern region (NOAA 4680) at 20 cm (total intensity and circular polarization), together with Hα photographs (SPO) and Kitt Peak magnetograms. Right circular polarization is white, left is black. The field of view is 350″ by 320″

In addition to the active region emission a diffuse, spread-out component is observed in the southern hemisphere, West of region 4682. Within this diffuse component several plage-associated sources are observed. One of them (marked with an arrow on the figure) is associated with a patch of Hα plage in the middle of a long filament. Another noteworthy discrete source is located in the western hemisphere (also marked with an arrow on Fig. 1), quite far from the active regions; it is compact and is associated with a small bright plage and a bipolar magnetic region. It is still visible on July 31, but from August 1 onwards it goes outside the field of view of the maps.

4. Active region 4680

This active region was located near the equator (latitude 5° North) and was observed in the longitude range of 31E to 20W. It extended over more than 20° in longitude and was in its decay phase during the observing period. L-band images in Stokes parameters I and V together with SPO Hα photographs and KPNO magnetograms of the region are shown in Fig. 2.

In Hα the region consists of a prominent filament running NE to SW, some other minor filaments and a prominent plage. The preceding spot is visible in Hα on July 30 and 31, but practically disappears from August 1. Spot drawings obtained from SGD show the presence of small spots or pores during the entire observing period. The magnetic structure is complex at the beginning of the period, with opposite polarity islands in the preceding part of the region; it became simpler by August 3.

The L-band emission during July 30 - August 2 consists of 3 components (*A*, *B*, *C* from east to west) and a diffuse background. The strongest component is *B*, which is located above the neutral line near the southern tip of the long filament, in a region of strong magnetic field gradient and strong magnetic field; it is therefore likely that it is due to free-free emission from compact coronal loops. The component *C* is located above the decaying spot; however it is weak and is probably associated with the plage surrounding the spot rather than with the spot itself; it increases in intensity on August 1 but on August 2 it is weaker and barely visible on August 3. The component *A* is associated with the plage of the following polarity; there is a significant increase in

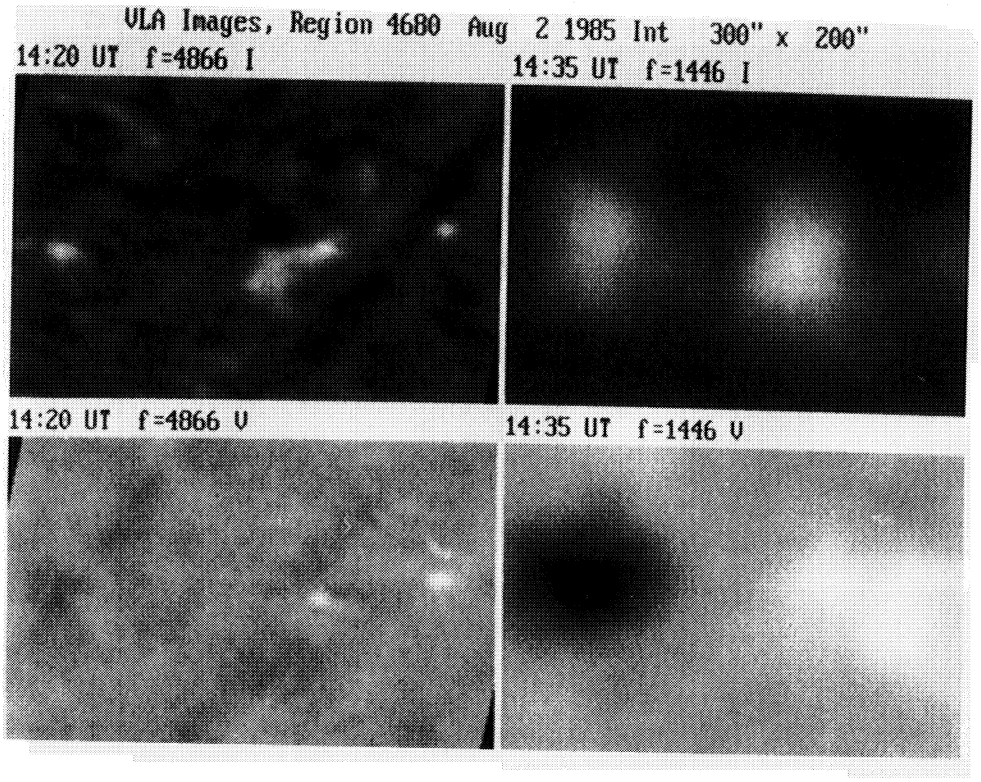

Fig. 3. 6 and 21 cm VLA maps of NOAA region 4680 obtained on August 2, 1985

its intensity on August 2. There is no obvious association of any of the components with the main body of the filament, which runs along a "corridor" of reduced emission between the sources *A* and *B*.

On August 3 only two sources are visible with no diffuse component. The absence of the diffuse component may be an instrumental effect (probably caused by lack of short baselines) since no diffuse component is observed in the southern region either. The two sources are identified with the components *A* and *B* of the previous days, while the component *C* does not show up as a discrete source. Short period maps (~20 min) showed that the component *B* faded and then reappeared, attributed to the large scale changes caused by a filament eruption (Kundu et al. 1989).

Near the central meridian passage (August 1) the region as a whole shows a clear bipolar structure in the V maps, with the sense of polarization as expected from the polarity of the photospheric magnetic field. The individual components are not bipolar, except for the strongest component *B*. As the region moves across the solar disk the large scale polarization structure changes due to wave propagation effects (Zheleznyakov 1970; Kundu & Alissandrakis 1984; Gelfreikh et al. 1987). The dominant sense of circular polarization corresponds to the magnetic polarity closer to the center of the disk; thus the right circularly polarized region (white in Fig. 2) dominates before August 1 and the left (black in Fig. 2) dominates after that date. These effects cause the apparent shift of the line of zero circular polarization as the region moves from close to the limb towards the center of the disk.

The only observations of region 4680 in the C-band were obtained on August 2, for a short period of about 1 hour (Fig. 3). The total intensity map shows three compact (~10″) sources, *a*, *b* and *c* from east to west. The source *b* is located at the west edge of a larger emission region, however no diffuse component of the size of the active region is visible; this is apparently due to the lack of short baseline spacings at this frequency. All three sources are located within the bulk emission of the L-band sources *A*, *B* and *C*.

A comparison of the positions of the sources with sunspot drawings from Solar Geophysical Data (SGD) shows that source *c* and the compact component of *b* are associated with small spots or pores, while there is no such association for the source *a*. Moreover these compact sources are ~50% polarized in the right hand circular sense, which is another indication of their sunspot-related origin. However, their polarization is not as high as one would expect if they were due to 3rd harmonic emission (~100%); emission at the second harmonic can account for the observed polarization, but it requires a magnetic field of at least 1200 G, which is rather unlikely for pores of that size (the 3rd harmonic requires only 600 G).

5. Active region 4682

Figure 4 shows the VLA L-band images of NOAA region 4682 in Stokes I and V along with Hα photographs (SPO) and longitudinal and transverse magnetic field images (KPNO, MSFC, Meudon). This particular region has been the subject of many investigations since it was observed extensively by the HRTS instrument during the Spacelab-2 mission (Kjeldseth-Moe et al. 1988; Dere et al. 1990). It is a mature active region with a well developed, almost axially symmetric preceding spot of negative magnetic polarity and a well developed bipolar magnetic structure which shows best on the KPNO magnetogram of August 3. There are, however, a few opposite polarity islands in the vicinity of the main spot, primarily in the north side. Note that the opposite polarity region, adjacent to the spot at its south-east side in the magnetograms of July 30 and 31, is due to the inclination of the penumbral field lines. This was verified through force-free

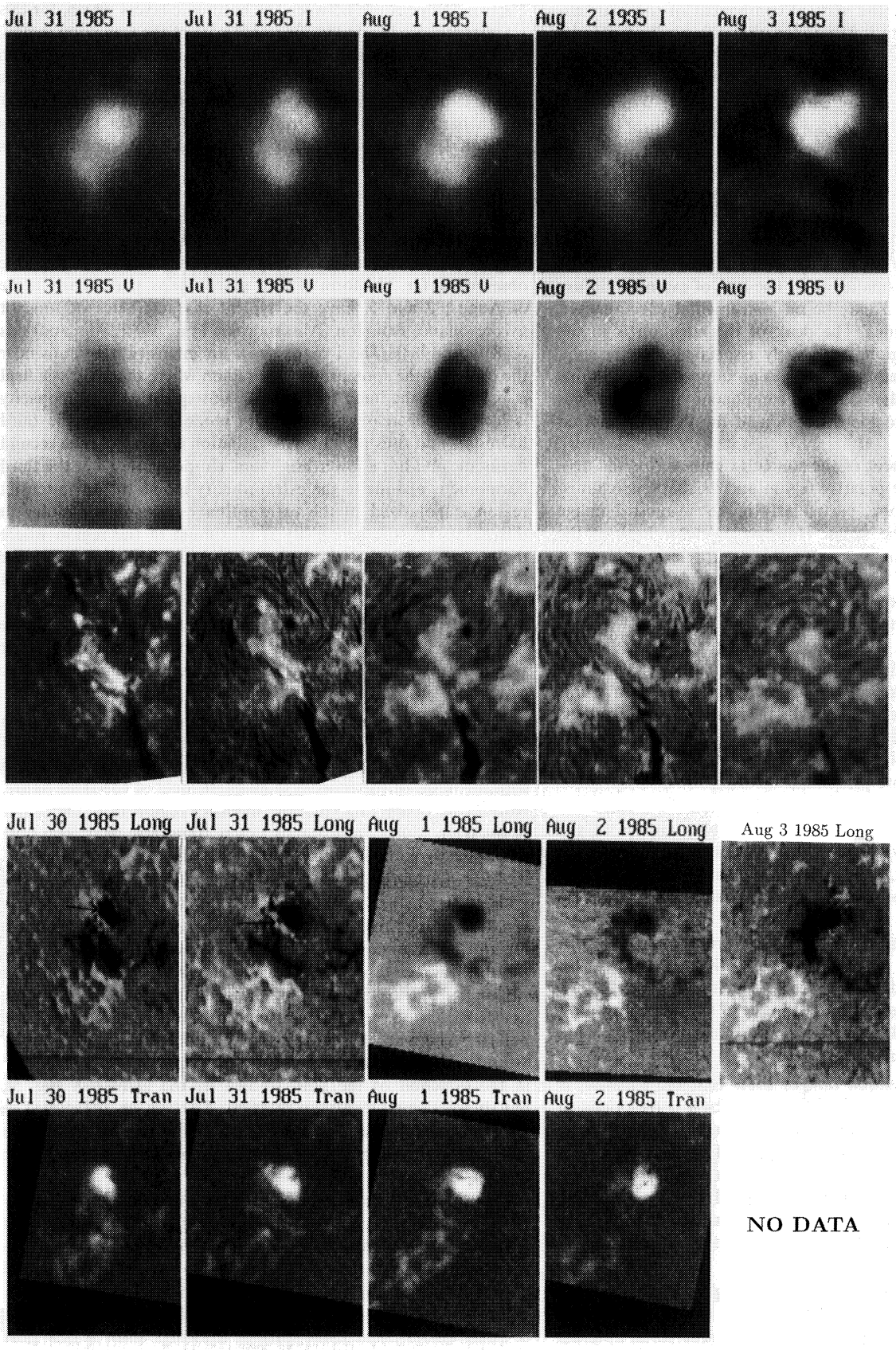

Fig. 4. Daily VLA maps of the Southern region (NOAA 4682) at 21 cm together with Hα photographs (SPO), longitudinal magnetograms (MSFC: August 1; KPNO: July 30-31, August 2; Meudon: August 2) and transverse magnetograms (MSFC). The field of view is 250″ by 350″

model computations of the vertical component of the magnetic field; the same computations verified that the positive polarity region north-east of the spot in the July 31 magnetogram is real.

It is interesting to note that the orientation of the dipole field of the region is highly inclined with respect to the E-W direction, being oriented almost N-S. Along the principal neutral line unstable filament-like structures developed occasionally (Schmieder et al. 1989), while a long filament was observed in Hα along the southern extension of the principal neutral line. The filament showed partial disruption on August 3 (Kundu et al. 1989).

The L-band maps show extended emission from the entire active region from July 30 to August 2, while on August 3 the emission is limited to a smaller area. The lack of extended diffuse component on August 3 may be an instrumental effect, caused by lack of short baselines. The peak of the emission is in the northern part of the region. It is clearly associated with the spot, indicating that the g-r mechanism plays an important role in this case. The absence of the southern component on August 3 is real, probably related to the disruption of the filament referred to earlier.

The diffuse component of the source extends across the neutral line to the opposite polarity region and its shape is reminiscent of a large scale loop, particularly on the August 2 image which is the best of the series. However, a closer look at the images gives two arguments against this interpretation. The first is the close similarity of the shape of the large scale emission with the underlying Hα plage; note in particular the negative polarity region that starts near the spot and extends south and west like a spiral arm or a spur. Similarly, the south part of the L-band source follows the outline of the positive polarity region, while a slight depression in the emission is seen along the neutral line. The second argument comes from the fact that the source retains its shape as it crosses the solar disk, which indicates a relatively flat and low structure; if it were a large loop, perspective effects would have made it more prominent far from the disk center.

On August 3 the north part of the L-band source is double peaked. The two peaks correspond to the two sources of the C-band map (see below), which shows that whatever caused the appearance of the weak, 100% polarized 6 cm source extends up to the level of formation of the 21 cm emission. As in the case of the region 4680, the southern component of the region 4682 also faded and reappeared on August 3, almost in phase with the western component of the region 4680 (Kundu et al. 1989). It has been speculated that large scale magnetic interconnections permitted the two regions, separated by 20°in latitude, to respond similarly to an external energy or mass source involved in the disruption of the filament.

The circular polarization images show that the emission is polarized predominantly in the left sense, which corresponds to the magnetic polarity of the sunspot. The left sense of polarization extends over the neutral line to the region of opposite magnetic polarity and only a small part of that region is polarized in the right circular sense. This can be understood in terms of wave propagation effects, which displace the position of the radio "neutral line" (i. e. the line of zero circular polarization) towards the limb.

It is interesting to note that the spot region itself is weakly polarized and that the peak of Stokes V is located near the middle of the active region. These properties can be understood in terms of gyroresonance emission: The low value of V above the spot is due to the high opacity of the harmonics that emit the ordinary and extraordinary modes, combined with the small difference in electron temperature between the harmonic layers which, for this wavelength, are located in the upper part of the transition region. The V peak is associated with the spur-shaped plage region which was mentioned above; it is plausible that the megnetic field is strong enough to produce optically thin emission at the third or fourth harmonics of the gyrofrequency. At 21 cm this requires 170 and 130 Gauss respectively, while the photospheric field is about 400 Gauss.

The C-band observations do not have sufficiently small baselines to show the large scale, plage associated emission. In spite of that, the images obtained on July 31, August 2 and August 3 (Fig. 5) are one of the best examples of sunspot-associated source observed so far. The form of the I and V maps, particularly those of August 2 and 3, have the typical characteristics of sunspot gyroresonance emission (Alissandrakis et al. 1980; Alissandrakis & Kundu 1984). The I maps show an intensity minimum near the center of the spot, around the region where the magnetic field is parallel to the line of sight and, consequently, the g-r opacity is low; this decreases the ordinary mode emission of the third harmonic and thus the ordinary radiation comes from the second harmonic and has a lower brightness temperature. Since the third harmonic is opaque to the extraordinary mode, the low intensity region is polarized in the extraordinary sense (left circular in this case). The total intensity is maximum in the region where the magnetic field has the highest inclination with respect to the line of sight, i. e. towards the limb; thus the source is crescent shaped, with the crescent oriented almost parallel to the limb. A second region of high circular polarization is observed at the limbward edge of the spot, where the magnetic field is too low for second harmonic emission, but strong enough for third harmonic emission.

A direct consequence of the dependence of the gyroresonance emission on the angle between the magnetic field and the line of sight is the close similarity of the total intensity maps of Fig. 5 with the maps of the transverse magnetic field of the same figure. Note in particular that the low intensity region near the center of the 6 cm source corresponds to low transverse field; also note the crescent shape of both 6 cm and transverse field images.

The above description assumes a cylindrically symmetric spot with a current-free magnetic field. The VLA images do show small deviations from this picture. For example, it is difficult to identify the low intensity region on August 2 (it is located near the diskward edge of the source); moreover there is enhanced emission from the east side of the spot. The latter is probably associated to the presence of a small region of opposite magnetic polarity. The map of August 2 shows another deviation from the "standard" model: the peak of the total intensity is not located in the direction of the limb (shown by the arrows in Fig. 5), but shows a small clockwise rotation. This can be interpreted in terms of a force-free magnetic field (cf. Alissandrakis & Kundu 1984), with the electric current flowing parallel to the magnetic field.

The August 3 images show that a new source emerged, southeast of the main source; it had a lower intensity but was almost 100% circularly polarized. These characteristics indicate g-r emission at the third harmonic. The source is located above a local enhancement of the photospheric longitudinal magnetic field, marked with an arrow on the longitudinal magnetogram in Fig. 5. Solar Geophysical Data sunspot drawings show a new pore at the same location. Since this region did not exist on August 2, the new region along with the photospheric field must have emerged during the night of August 2. The new magnetic flux is

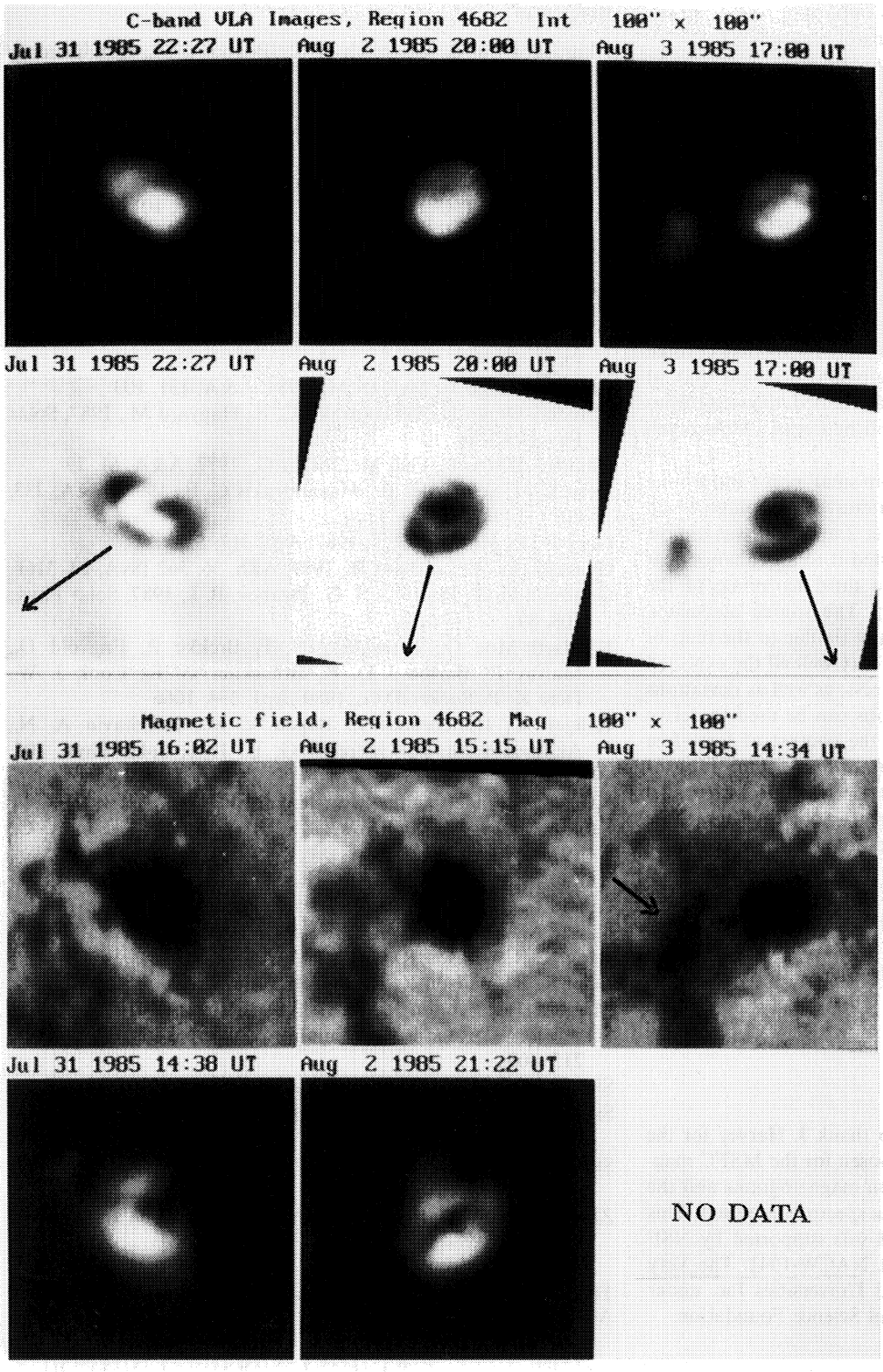

Fig. 5. VLA maps of the sunspot associated source in NOAA region 4682 at 6 cm obtained on July 31, August 2 and August 3, 1985, together with longitudinal and transverse magnetograms. The arrows on the circular polarization maps show the direction of the limb. The arrow on the longitudinal magnetogram of August 3 points to a new magnetic region, associated with the weak 6 cm source

also responsible for the double peaked structure of the L-band source which was discussed above.

6. Summary and conclusions

The simultaneous VLA observations at 6 and 20 cm which were presented in this work provide complementary information about the structure and the physical conditions in the transition region and low corona above active regions. The 6 cm maps best show the sunspots, while the 20 cm maps best show the large scale structure. This has both an instrumental (lack of short baselines) and a physical basis: the increased efficiency of free-free emission at longer wavelengths, combined with the relatively steady emission from the gyroresonance process, decrease the contrast between regions of large (sunspot) and moderate (plage) mag-

netic field. Gyroresonance still plays an important role at 20 cm, as was demonstrated by the observations of region 4682.

The current view about active region emission is that it occurs in large scale loops. The present observations do not fully corroborate this view. We have one case of emission associated with a neutral line, and this was a compact source. If it is loop-associated, the loops must be small and they are not resolved. Other possibilities, such as current sheets cannot be excluded, in the lack of reliable spectral information. All other sources had a close association with the chromospheric plage and, moreover, showed no changes produced by perspective effects as the regions crossed the solar disk. Thus the present data are closer to the more traditional view that the large scale 20 cm emission comes primarily from plage regions. This does not mean that coronal loops do not contribute at all to the emission; it means that, at least in the case of the two active regions studied, their contribution is small. It is possible that they will be better visible much closer to the limb.

We observed 6 cm emission both from small pores and from a well developed sunspot. Of particular interest is the source which appeared in region 4682 between August 2 and 3; it was almost 100% polarized at 6 cm and we attributed it to an enhancement of the magnetic field that brought the third harmonic of the gyrofrequency in the transition region. The source associated with the well developed sunspot was very similar to the map of the transverse magnetic field; it showed very well all the expected characteristics of the gyroresonance process, as well as deviations from the idealized model. Such deviations can be used to derive information about electric currents, in the context of force-free magnetic field models. For the interpretation of the position of maximum intensity we need to introduce electric currents parallel to the magnetic field. It is interesting to note that the same conclusion was reached by Schmieder et al. (1989) and by Dere et al. (1990) for the same spot, on the basis of the orientation of chromospheric and transition region (C IV) fibrils and on the basis of the azimuthal component of the chromospheric Evershed flow. This verifies that the microwave observations are a very important diagnostic of the transition region and the low corona.

Acknowledgements. The authors wish to thank J. Harvey for the KPNO magnetograms, E. Tandberg-Hansen for the MSFC magnetograms, B. Schmieder for the Meudon magnetograms and the Sacramento Peak Observatory for the Hα spectroheliograms. This research at the University of Maryland was supported by NSF grant ATM 90-19893 and NASA grant NACW-1541. The Very Large Array is operated by Associated Universities Inc. under cooperative agreement with the National Science Foundation.

References

Akhmedov Sh. B., Gelfreikh G. B., Bogod V. M., Korzhavin A. N., 1982, Solar Phys., 79, 41
Akhmedov Sh. B., Borovik V. N., Gelfreikh G. B., Bogod V. M., Korzhavin A. N., Petrov Z. E., Dikij V. N., Lang K. R., Willson R. F., 1986, ApJ, 301, 460
Alissandrakis C. E., 1980, in: Radio Physics of the Sun, eds M. R. Kundu, T. Gergely, Reidel, Dordrecht, p. 101
Alissandrakis C. E., Kundu M. R., 1982, ApJ, 253, L49
Alissandrakis C. E., Kundu M. R., 1984, A&A, 139, 271
Alissandrakis C. E., Kundu M. R., Lantos P., 1980, A&A, 82, 30
Chiuderi-Drago F., Bandiera R., Falciani R., Antonucci E., Lang K. R., Willson R. F., Shibasaki K., Slottje K., 1982, Solar Phys., 80, 71
Chiuderi-Drago F., Melozzi M., 1984, A&A, 131, 103
Chiuderi-Drago F., Alissandrakis C. E., Hagyard M., 1987, Solar Phys., 112, 89
Chiuderi-Drago F., Felli M., Tofani G., 1977, A&A, 61, 79
Dere K. P., Schmieder B., Alissandrakis C. E., 1990, A&A, 233, 207
Gary D. E., Hurford G. J., 1987, ApJ, 317, 552
Gelfreikh G. B., Lubishev B., 1979, AZh, 56, 562 (SvA, 23, 316)
Gelfreikh G. B., Peterova N. G., Ryabov, B. I., 1987, Solar Phys., 108, 89.
Kjeldseth-Moe O., Brynildsen N. F, Brekke P., Engvold O., Maltby P., Bartoe J.-D. F., Brueckner G. E., Cook J. W., Dere K. P., Socker D.G., 1989, ApJ, 334, 1066
Krüger A., Hildebrandt J., Bogod V. M., Korzhavin A. N., Akhmedov Sh. B., Gelfreikh G. B., 1986, Solar Phys., 105, 111
Krüger A., Hildebrandt J., Fürstenberg F., 1985, A&A, 143, 72
Kundu M. R., Alissandrakis C. E., Bregman J. D., Hin A. C., 1977, ApJ, 213, 278
Kundu M. R., Alissandrakis C. E., 1984, Solar Phys., 94, 249
Kundu M. R., Schmahl E. J., Rao A. P., 1981, A&A, 94, 72
Kundu M. R., Schmahl E. J., Fu Q.-J., 1989, ApJ, 336, 1078
Lang K. R., Willson R. F., 1982, ApJ, 255, L111
Lang K. R., Willson R. F., Rayrole J., 1982, ApJ, 258, 387
McConnel D., Kundu M. R., 1983, ApJ, 269, 698
Schmieder B., Raadu M., Démoulin P., Dere K.P., 1989, A&A, 213, 402
Shevgaonkar R. K., Kundu M. R., 1985, Solar Phys., 98, 119
Siarkovski M., Sylwester J., Jakimiek J., Bently R. D., 1989, Solar Phys., 119, 189
Strong K. T., Alissandrakis C. E., Kundu M. R., 1984, ApJ, 277, 865
Zheleznyakov V. V., 1970, Radio Emission of the Sun and Planets, Pergamon Press, Oxford

This article was processed by the author using Springer-Verlag LaTeX A&A style file 1990.